C–C Double- and Triple-Bond Formation from Reactions of B Atoms with CO: Experimental and Theoretical Characterization of OBBCCO and OBCCBO Molecules in Solid Argon

Mingfei Zhou,*[a] Ling Jiang,[b] and Qiang Xu*[b]

Abstract: Reactions of boron atoms with CO molecules in solid argon form the following boron carbonyl species (which have been reported earlier): BCO, BBCO, OCBBCO, $B(CO)_2$, and $B_4(CO)_2$. The OCBBCO molecule underwent a photochemical rearrangement where CO was activated to form the OBBCCO and OBCCBO molecules. The new molecules were identified on the basis of isotopic IR studies with ^{10}B, ^{11}B, $^{13}C^{16}O$, $^{12}C^{18}O$, and carbon dioxide mixtures in addition to comparison with quantum-chemical calculations of isotopic frequencies. Theoretical analyses showed that the OBBCCO and OBCCBO molecules are linear with C–C double and triple bonding, respectively, and lie at a much lower energy than the linear OCBBCO structure.

Keywords: boron carbonyls · CO activation · density functional calculations · IR spectroscopy · matrix isolation

Introduction

Carbon monoxide activation and reduction are important in a great many industrial processes, such as hydroformylation, alcohol synthesis, and acetic acid synthesis.[1] The reactions of carbon monoxide with transition-metal atoms have been extensively studied. A variety of transition-metal–carbonyl complexes have been experimentally characterized, and theoretical studies of the electronic structures and bonding of these complexes have been carried out.[2] Recent infrared spectroscopic investigations of the reactions of laser-ablated early transition-metal and actinide metal atoms with CO have demonstrated CO activation through transition-metal– and actinide-metal–carbonyl complexes.[3–6] The monocarbonyls of Nb, Th, and U can be isomerized to form the inserted carbide-oxide molecules by using visible-light irradiation. The dicarbonyls of the Ti group, V group, and the actinide metals Th and U undergo photo-induced isomerization to form the OMCCO molecules (M = Ti, Zr, Hf, V, Nb, Ta, U, and Th) with visible or UV photons. The OMCCO molecules can undergo a further photochemical rearrangement to form the $OTh(\eta^3\text{-}CCO)$ or $(\eta^2\text{-}C_2)MO_2$ molecules (M = Nb, Ta, and U) with UV photons.

The spectra, structures, and bonding of main-group carbonyls, particularly the Group 13 metal carbonyls, have also gained considerable attention, but no CO-activation reaction was reported in the reactions of main-group elements with CO.[7–18] We have characterized boron–carbonyl species such as BBCO,[19] OCBBCO,[20] and $B_4(CO)_2$[21] as products from the reactions of boron atoms with CO in solid argon. Similar to $[HGa{\equiv}GaH]^{2-}$,[22] OCB≡BCO exhibits some degree of boron–boron triple bonding.[20] $B_4(CO)_2$, with a four-membered B_4 ring, was characterized as a new σ–π diradical, which represents a remarkable example of aromaticity with three π electrons.[21] In this paper, we report a combined matrix-isolation, spectroscopic, and theoretical study of the photochemical formation of OBBCCO and OBCCBO from the boron–carbonyl species.

Experimental Section

The experiments for laser ablation and matrix-isolation spectroscopy were similar to those used previously.[23] Briefly, the Nd:YAG laser fundamental (1064 nm, 10 Hz repetition rate, 10 ns pulse width) was focused on the rotating boron target. The laser-ablated boron atoms were co-deposited with CO in excess argon onto a CsI window cooled to 7 K by means of a closed-cycle helium cryostat. The matrix-gas deposition rate was typically 2–4 mmol per hour. Carbon monoxide, $^{13}C^{16}O$ (99%), and $^{12}C^{18}O$ (99%) were used to prepare the CO/Ar mixtures. Natural-abun-

[a] Prof. M. Zhou
Department of Chemistry
Shanghai Key Laboratory of Molecular Catalysts and Innovative Materials
Fudan University, Shanghai 200433 (P.R. China)
Fax: (+86) 21-656-43532
E-mail: mfzhou@fudan.edu.cn

[b] L. Jiang, Dr. Q. Xu
National Institute of Advanced Industrial Science and Technology (AIST)
Ikeda, Osaka 563-8577 (Japan)
Fax: (+81) 727-51-9629
E-mail: q.xu@aist.go.jp

 DOI: 10.1002/chem.200400474

dance boron (^{10}B 19.8%, ^{11}B 80.2%) and ^{10}B-enriched (97%) targets were used in different experiments. In general, matrix samples were deposited for one to two hours. After sample deposition, IR spectra were recorded on a BIO-RAD FTS-6000e spectrometer at 0.5 cm^{-1} resolution using a liquid-nitrogen-cooled HgCdTe (MCT) detector for the spectral range of 5000–400 cm^{-1}. Samples were annealed at different temperatures and subjected to broad-band irradiation ($\lambda > 250$ nm) by using a high-pressure mercury arc lamp (Ushio, 100 W).

Computational methods: Quantum-chemical calculations were performed to predict the structures and vibrational frequencies of the observed reaction products using the Gaussian 98 program.[24] The Becke three-parameter hybrid functional with the Lee–Yang–Parr correlation correction (B3LYP) was used.[25,26] Comparative ab initio calculations were also performed at the CCSD(T) level.[27] The 6-311+G(d) basis sets were used for B, C, and O atoms.[28] Geometries were fully optimized at both levels of theory, while vibrational frequencies were calculated only at the B3LYP level with analytical second derivatives.

Results and Discussion

Infrared spectra: A series of experiments have been carried out with different CO concentrations (from 0.025 to 0.5% in argon) and laser energies (from 5 to 20 mJ pulse^{-1}). Figure 1

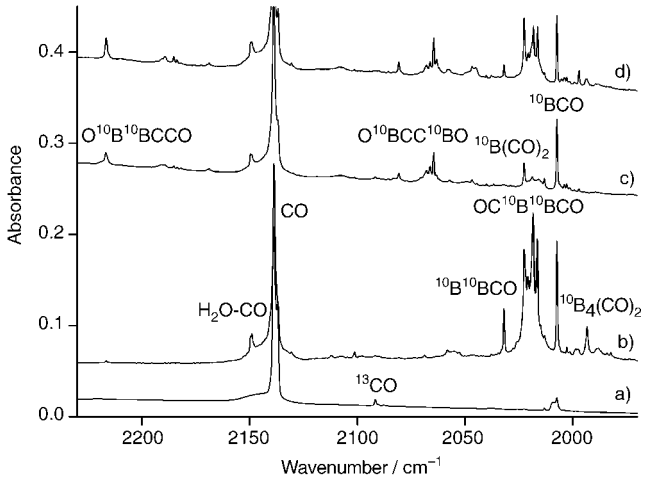

Figure 1. Infrared spectra in the 2230–1970 cm^{-1} region from co-deposition of laser-ablated boron atoms (^{10}B-enriched, 97%) with 0.1% CO in Ar: a) 1 h of sample deposition at 7 K; b) after annealing to 34 K; c) after 20 min of broad-band irradiation; d) after annealing to 38 K.

shows the infrared spectra in the 2230–1970 cm^{-1} region containing one absorption band for each reaction product with ^{10}B and 0.1% CO in argon. The new product absorption bands are listed in Table 1. After deposition (Figure 1a), the ^{10}BCO absorption bands (1148.1, 2007.3, 2291.1, 3139.1, 3992.7 cm^{-1})[11,29] were observed together with a CO absorption band at 2138.3 cm^{-1}. After annealing the sample (7–34 K, Figure 1b), the BCO absorption bands increased and the ^{10}B^{10}BCO (2031.9, 1524.5 cm^{-1}),[19] ^{10}B(CO)$_2$ (2022.5 cm^{-1}),[29] OC^{10}B^{10}BCO (2016.4, 1116.5 cm^{-1}),[20] and ^{10}B$_4$(CO)$_2$ (1993.3, 1365.8 cm^{-1})[21] absorption bands were produced. Broad-band irradiation (Figure 1c) decreased the BCO and B(CO)$_2$ bands, destroyed the BBCO and OCBBCO bands, and produced new bands at 2216.6, 2064.6, 934.0, and 490.1 cm^{-1}. These new bands sharpened on further annealing of the sample to 38 K (Figure 1d).

Table 1. Infrared absorption bands [cm^{-1}] from co-deposition of laser-ablated boron atoms with CO in solid argon.

^{12}C^{16}O[a]	^{13}C^{16}O	^{12}C^{18}O	Assignment	
2216.6	2140.0	2197.8	O^{10}B^{10}BCCO	CO str.[b]
2215.7	2147.0	2196.9	O^{11}B^{10}BCCO	
2209.0	2144.3	2190.4	O^{11}B^{11}BCCO	
2064.6	2062.1	2034.9	O^{10}BCC^{10}BO	*as*-BO str.[b]
2040.2	2034.5	2010.1	O^{10}BCC^{11}BO	
1999.3	1996.8	1965.6	O^{11}BCC^{11}BO	
1942.7	1936.1	1916.9	O^{10}BCC^{11}BO	*s*-BO str.[b]
934.0	912.0	919.5	O^{10}BCC^{10}BO	*as*-BC str.[b]
930.9	909.5	917.1	O^{10}BCC^{11}BO	
928.1	906.8	914.9	O^{11}BCC^{11}BO	
490.1	486.7	487.5	O^{10}BCC^{10}BO	*as*-OBC bend.[b]
480.7	477.0	478.1	O^{10}BCC^{11}BO	
473.7	470.2	471.1	O^{11}BCC^{11}BO	

[a] Two matrix trapping sites were observed for the fundamentals of OBCCBO and only the major site absorption bands are listed. [b] Abbreviations: str. = stretching mode, bend. = bending mode, *as* = asymmetric, *s* = symmetric.

Similar experiments were also carried out with a natural-abundance boron target. The spectra in the 2230–1920 cm^{-1} region are shown in Figure 2. Again, the BCO absorption bands (^{10}BCO and ^{11}BCO with approximately 1:4 relative intensities) were observed on sample deposition (Figure 2a), and markedly increased on annealing (7–34 K, Figure 2b). The absorption bands of different BBCO, B(CO)$_2$, OCBBCO, and B$_4$(CO)$_2$ isotopomers appeared on annealing to 34 K, as reported earlier.[19–21,29] New absorption bands at 2215.7, 2209.0, 2040.2, 1999.3, 1942.7, 930.9, 928.1, 480.7, and 473.7 cm^{-1} were produced after 15 min of broad-band irradiation (Figure 2c). Another 15 min of irradiation (Figure 2d) slightly increased the 2040.2, 1999.3, 1942.7, 930.9, 928.1, 480.7, and 473.7 cm^{-1} bands at the expense of the 2215.7 and 2209.0 cm^{-1} bands. Isotopic carbon monoxides (^{13}C^{16}O and ^{12}C^{18}O) and mixtures (^{12}C^{16}O + ^{13}C^{16}O and ^{12}C^{16}O + ^{12}C^{18}O)

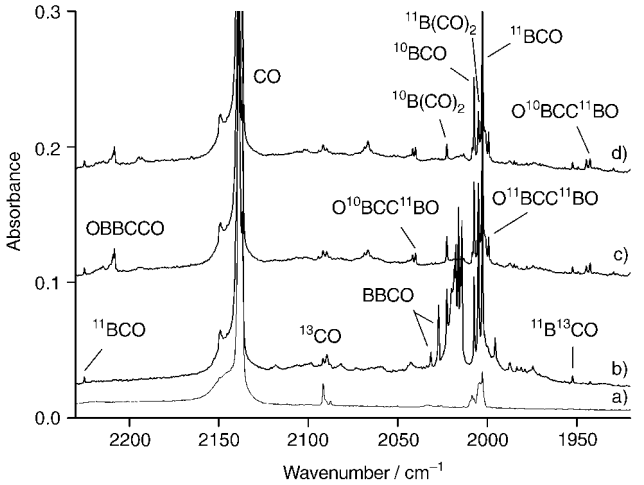

Figure 2. Infrared spectra in the 2230–1920 cm^{-1} region from co-deposition of laser-ablated boron atoms (natural abundance) with 0.1% CO in Ar: a) 1 h of sample deposition at 7 K; b) after annealing to 34 K; c) after 15 min of broad-band irradiation; d) after 30 min of broad-band irradiation.

were employed for product identification by observing isotopic shifts and splittings. The isotopic counterparts are also listed in Table 1. Figures 3, 4, and 5 (see later) show the spectra in selected regions using different isotopic samples after broad-band irradiation.

Calculation results: Quantum-chemical calculations were performed on the potential product molecules. The optimized structures at both the B3LYP6-311+G* and CCSD(T)/6-311+G* levels are shown in Figure 6 (see later). The vibrational frequencies and intensities calculated at the B3LYP6-311+G* level are listed in Table 2. Table 3 provides a comparison of observed and calculated isotopic frequency ratios for the observed vibrational modes.

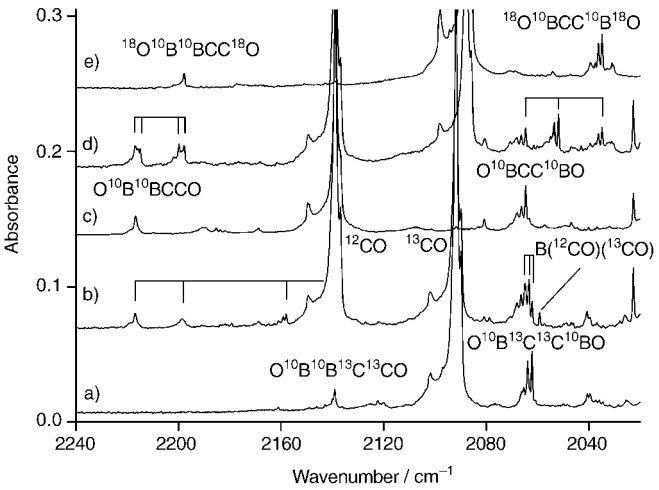

Figure 3. Infrared spectra in the 2240–2020 cm^{-1} region from co-deposition of laser-ablated boron atoms (^{10}B-enriched, 97%) with different isotopic CO samples in excess argon. Spectra were recorded after sample deposition followed by annealing (34 K) and 20 min of broad-band irradiation: a) 0.1% ^{13}CO; b) 0.05% ^{12}CO + 0.05% ^{13}CO; c) 0.1% ^{12}CO; d) 0.05% C^{16}O + 0.05% C^{18}O; e) 0.1% C^{18}O.

Table 2. Vibrational frequencies [cm^{-1}] and intensities [km mol^{-1}] of $O^{10}B^{10}BCCO$ and $O^{10}BCC^{10}BO$ molecules calculated at the B3LYP6-311+G* level.

	Frequency (intensity, mode)
OBBCCO ($^1\Sigma^+$)	2303.9 (1872, σ), 2113.3 (376, σ), 1908.8 (77, σ), 1138.3 (4, σ), 622.2 (54, π), 514.4 (6, π), 486.3 (1, σ), 246.4 (56, π), 81.6 (8, π)
OBCCBO ($^1\Sigma_g^+$)	2347.8 (0, σ_g), 2123.6 (811, σ_u), 2045.3 (0, σ_g), 982.1 (15, σ_u), 561.7 (0, π_g), 525.0 (0, σ_g), 511.5 (166, π_u), 265.5 (0, π_g), 90.7 (27, π_u)

Molecule OBBCCO: We have recently characterized a boron–boron triple-bonded OCBBCO molecule.[20] The present experiments provide evidence for two other products of $B_2C_2O_2$ stoichiometry. The band at 2216.6 cm^{-1} was produced following broad-band irradiation; this band split into a doublet at 2215.7 and 2209.0 cm^{-1} with approximately 1:4 relative intensities when the natural-abundance boron target was used, which indicated that this vibration mainly involves one boron atom and is slightly coupled with another non-equivalent boron atom. The 2216.6 cm^{-1} band shifted to 2140.0 cm^{-1} with $^{13}C^{16}O$ and to 2197.8 cm^{-1} with $^{12}C^{18}O$, giving the isotopic frequency ratio of 1.0358 for $^{12}C/^{13}C$ and 1.0086 for $^{16}O/^{18}O$. These ratios are significantly larger and smaller, respectively, than diatomic CO ratios, suggesting strong coupling with another C atom. The band position and isotopic frequency ratios imply the involvement of a CCO subunit in the molecule (the C–O stretching mode of CCCO was observed at 2242.6 cm^{-1} in solid argon, with isotopic ratios: $^{16}O/^{18}O$ 1.0083, $^{12}C_3O/^{12}C^{13}C_2O$ 1.0316; the C–O stretching mode of H_2CCO was observed at 2142.1 cm^{-1} in solid argon: $^{16}O/^{18}O$ 1.0126, $^{12}C/^{13}C$ 1.0298).[30] In the mixed $^{12}C^{16}O + ^{13}C^{16}O$ experiment (Figure 3b), two intermediate components at 2198.5 and 2159.2 cm^{-1} were clearly resolved, while in the mixed $^{12}C^{16}O + ^{12}C^{18}O$ experiment (Figure 3d), a quartet at 2216.6, 2214.9, 2199.8, and 2197.8 cm^{-1} with approximately 1:1:1:1 relative intensities was observed. These observations demonstrated that two non-equivalent B atoms, two non-equivalent C atoms, and two non-equivalent O atoms were involved in this vibrational mode. Accordingly, we assigned the 2216.6 cm^{-1} band to the C–O stretching vibration of the $O^{10}B^{10}BCCO$ molecule.

Quantum-chemical calculations were performed to support the experimental assignment. Similar to OCBBCO, which has a singlet ground state with a linear structure, we found that OBBCCO also has a singlet ground state ($^1\Sigma^+$) with a linear structure, as shown in Figure 6 (see later). Our B3LYP6-311+G* calculations on $O^{10}B^{10}BCCO$ predicted a very strong C–O stretching mode at 2303.9 cm^{-1}. This predicted frequency deviates from the experimentally observed frequency by only 3.9%. The calculated isotopic frequency ratios—$^{10}B/^{11}B$ 1.0024, $^{12}C/^{13}C$ 1.0315, $^{16}O/^{18}O$ 1.0075—are in reasonable agreement with the experimental ratios—$^{10}B/^{11}B$ 1.0034, $^{12}C/^{13}C$ 1.0358, $^{16}O/^{18}O$ 1.0086 (see Table 3). It should be mentioned that the calculated $^{12}C/^{13}C$ ratio of $O^{10}B^{10}BCCO$ is lower than the experimental value, whereas the calculated $^{12}C/^{13}C$ ratio of $O^{11}B^{11}BCCO$ (1.0325) is higher than the experimental ratio (1.0302). This suggests that the C–O stretching mode of $OBB^{13}C^{13}CO$ is in anharmonic resonance with a combination of low-lying levels. The C–O stretching mode was predicted to have the largest IR intensity (1872 km mol^{-1} for $O^{10}B^{10}BCCO$). The B–O stretching vibration was predicted at 2113.3 cm^{-1} and is the second most intense mode; its calculated intensity is about

Table 3. Comparison of the observed and calculated isotopic frequency ratios of the $O^{10}B^{10}BCCO$ and $O^{10}BCC^{10}BO$ molecules.

	Mode	$^{10}B/^{11}B$		$^{12}C/^{13}C$		$^{16}O/^{18}O$	
		calcd	obsd	calcd	obsd	calcd	obsd
OBBCCO	CO str.[a]	1.0024	1.0034	1.0315	1.0358	1.0075	1.0086
OBCCBO	BO str.[a]	1.0334	1.0327	1.0011	1.0012	1.0152	1.0146
	BC str.[a]	1.0016	1.0064	1.0263	1.0241	1.0184	1.0158
	OBC bend.[b]	1.0346	1.0346	1.0069	1.0070	1.0053	1.0053

[a] str. = stretching mode. [b] bend. = bending mode.

20% of the C–O stretching mode. A weak band at 2080.3 cm^{-1} might be assigned to this mode, however, the isotopic shifts and splittings of this band are not clear due to weakness and band overlap, and definitive assignment is not possible. All the other modes were predicted to have very low IR intensities (Table 2).

In addition to OBBCCO, we computed other possible structural isomers, including the BOBCCO and OBCBCO isomers, which also involve non-equivalent B, C, and O atoms. Our calculations found that both BOBCCO and OBCBCO have singlet ground states with linear structures. These molecules were predicted to be 30 and 18 kcal mol^{-1} less stable than OBBCCO, respectively. None of these isomers were computed to have infrared spectral features that matched the observed frequencies.[31]

Molecule OBCCBO: The bands at 2064.6, 934.0, and 490.1 cm^{-1} in experiments with a ^{10}B-enriched target, and the bands at 2040.2, 1999.3, 1942.7, 930.9, 928.1, 480.7, and 473.7 cm^{-1} in experiments with a natural-abundance boron target appeared following broad-band irradiation and were assigned to a linear OBCCBO molecule. Each band has a minor site absorption that is 1–2 cm^{-1} higher. These bands can be grouped together on the basis of their growth/decay characteristics measured as a function of change of experimental conditions, suggesting that they are a result of different vibrational modes of the same molecule. The 2064.6, 2040.2, and 1999.3 cm^{-1} bands were assigned to the antisymmetric B–O stretching mode of the $O^{10}BCC^{10}BO$, $O^{10}BCC^{11}BO$, and $O^{11}BCC^{11}BO$ isotopomers, respectively. The relative intensities of these three absorption bands are consistent with two equivalent boron atom involvements. With natural-abundance boron, a vibrational mode, involving two equivalent boron atoms, will split into three absorption bands with approximately 1:8:16 relative intensities. The 2064.6 cm^{-1} band was shifted to 2062.1 cm^{-1} with $^{13}C^{16}O$ and to 2034.9 cm^{-1} with $^{12}C^{18}O$. The isotopic frequency ratios ($^{16}O/^{18}O$ 1.0146, $^{12}C/^{13}C$ 1.0012, $^{10}B/^{11}B$ 1.0327), are characteristic of a predominantly terminal B–O stretching vibration. As listed in Table 1, the 2040.2 and 1999.3 cm^{-1} bands exhibited very similar carbon-13 and oxygen-18 frequency shifts to that of the 2064.6 cm^{-1} band. In the mixed $^{12}C^{16}O+^{13}C^{16}O$ experiment (Figure 3b), a triplet was observed for the 2064.6 cm^{-1} band with an intermediate at 2063.3 cm^{-1}, indicating that two equivalent C atoms are involved in the mode. A similar triplet with an intermediate at 2051.9 cm^{-1} was also observed in the mixed $^{12}C^{16}O+^{12}C^{18}O$ experiment (Figure 3d), which indicates that two equivalent O atoms are involved. The symmetric B–O stretching mode of the linear $O^{10}BCC^{10}BO$ and $O^{11}BCC^{11}BO$ molecules is IR inactive, but the mode of $O^{10}BCC^{11}BO$ is IR active because of the reduced symmetry. In the experiment with a natural-abundance boron target, a weak band at 1942.7 cm^{-1} appeared following broad-band irradiation and tracked with the 2040.2 and 1999.3 cm^{-1} bands; this was assigned to the symmetric B–O stretching mode of $O^{10}BCC^{11}BO$.

The bands at 934.0, 930.9, and 928.1 cm^{-1}, and the bands at 490.1, 480.7, and 473.7 cm^{-1} were assigned to the antisymmetric B–C stretching and OBC bending vibrations of the $O^{10}BCC^{10}BO$, $O^{10}BCC^{11}BO$, and $O^{11}BCC^{11}BO$ isotopomers, respectively. The spectra shown in Figures 4 and 5 clearly

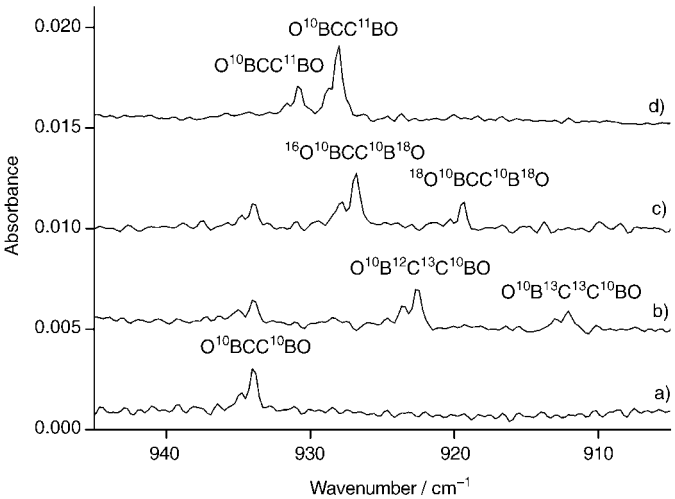

Figure 4. Infrared spectra in the 945–905 cm^{-1} region from co-deposition of laser-ablated boron atoms with CO in excess argon. Spectra were recorded after sample deposition followed by annealing (34 K) and 20 min of broad-band irradiation: a) 0.1% ^{12}CO, ^{10}B-enriched (97%); b) 0.05% ^{12}CO + 0.05% ^{13}CO, ^{10}B-enriched (97%); c) 0.05% $C^{16}O$ + 0.05% $C^{18}O$, ^{10}B-enriched (97%); d) 0.1% CO, natural-abundance boron.

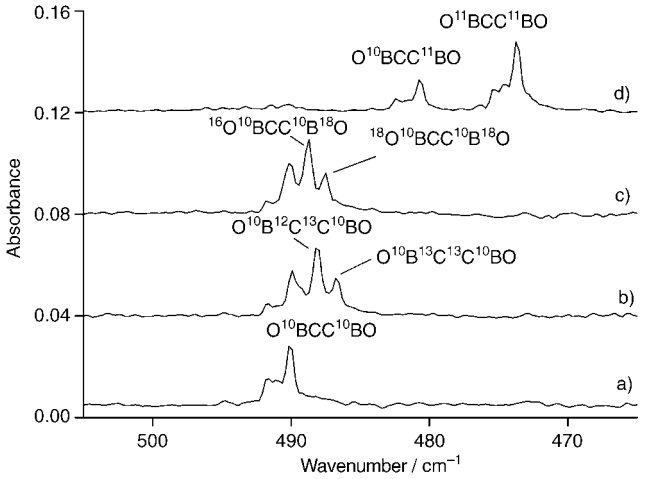

Figure 5. Infrared spectra in the 505–465 cm^{-1} region from co-deposition of laser-ablated boron atoms with CO in excess argon. Spectra were recorded after sample deposition followed by annealing (34 K) and 20 min of broad-band irradiation: a) 0.1% ^{12}CO, ^{10}B-enriched (97%); b) 0.05% ^{12}CO + 0.05% ^{13}CO, ^{10}B-enriched (97%); c) 0.05% $C^{16}O$ + 0.05% $C^{18}O$, ^{10}B-enriched (97%); d) 0.1% CO, natural-abundance boron.

demonstrate that two equivalent boron, two equivalent carbon, and two equivalent oxygen atoms are involved in these two vibrational modes. The 934.0 cm^{-1} band, for example, is shifted to 912.0 cm^{-1} with $^{13}C^{16}O$ and to 919.5 cm^{-1} with $^{12}C^{18}O$. A triplet at 934.0, 922.6, and 912.0 cm^{-1} with approximately 1:2:1 relative intensities was observed in the mixed $^{12}C^{16}O+^{13}C^{16}O$ spectrum (Figure 4b). Similarly, a triplet at 934.0, 926.9, and 919.5 cm^{-1} was observed in the mixed $^{12}C^{16}O+^{12}C^{18}O$ experiment (Figure 4c).

The assignment is strongly supported by quantum-chemical calculations. As shown in Figure 6, the OBCCBO molecule was predicted to have a closed-shell singlet ground

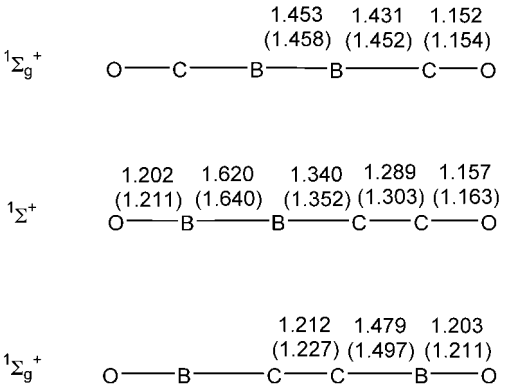

Figure 6. Optimized structures (bond lengths in angstroms) of the three $B_2C_2O_2$ isomers at the B3LYP6-311+G* and CCSD(T)/6-311+G* (in parentheses) levels.

state with a linear structure. There are thirteen vibrational fundamentals for linear OBCCBO, but only six of them are IR active. The antisymmetric B–O stretching (σ_u), B–C stretching (σ_u), and doubly degenerated OBC bending (π_u) vibrations for $O^{10}BCC^{10}BO$ were computed at 2123.6, 982.1, and 511.5 cm^{-1}, respectively, which should be multiplied by 0.972, 0.951, and 0.958, respectively, to reproduce the observed frequencies. This is in accord with the expected accuracy of B3LYP calculations.[32] The calculated intensity ratio of these three modes is 811:15:178, which is in good agreement with the experimental ratio of the band intensities of 0.089:0.002:0.022. Two other IR-active bending vibrations that are doubly degenerated were predicted at 90.7 cm^{-1}, which is outside the range of our spectrometer. The symmetric B–O stretching mode (σ_g) of $O^{10}BCC^{10}BO$ is IR inactive, but this mode of $O^{10}BCC^{11}BO$ was calculated at 2008.8 cm^{-1} with appreciable IR intensity (89 $km\,mol^{-1}$), completely consistent with the experiment. As listed in Table 3, the calculated $^{10}B/^{11}B$, $^{12}C/^{13}C$, and $^{16}O/^{18}O$ isotopic frequency ratios for the B–O stretching and OBC bending modes are in excellent agreement with the observed values, but the calculated $^{10}B/^{11}B$ ratio for the B–C stretching mode is smaller than the experimental value. This suggests the possibility of anharmonic resonance of the B–C stretching mode with the bending vibration, exhibiting a relatively larger $^{10}B/^{11}B$ isotopic effect. As a reference point, anharmonic resonance between the B–CO stretching mode and the bending mode was observed for the BCO molecule, which resulted in a larger deviation between the calculated and observed isotopic frequency ratios for the B–C stretching mode.[29]

The co-deposition of laser-ablated boron atoms with CO in excess argon produced BCO as the primary product. The BBCO, $B(CO)_2$, OCBBCO, and $B_4(CO)_2$ carbonyls were formed following sample annealing. As has been discussed,[20] OCBBCO was formed by BCO dimerization and not through B_2 reactions. The OBBCCO and OBCCBO absorption bands were produced following broad-band irradiation, during which those absorption bands for OCBBCO disappeared, indicating that OBBCCO and OBCCBO were formed by photo-induced isomerization of OCBBCO. The absorption bands for OBBCCO decreased on prolonged broad-band irradiation, during which the OBCCBO absorption bands still increased. These observations strongly suggest the successive photo-induced rearrangement of OCBBCO to OBBCCO and finally to OBCCBO, as shown in Equations (1) and (2):

$$OCBBCO + h\nu \rightarrow OBBCCO \quad (1)$$

$$OBBCCO + h\nu \rightarrow OBCCBO \quad (2)$$

Our B3LYP calculations indicate that these rearrangements are exothermic. All three $B_2C_2O_2$ isomers observed in the experiments are linear molecules. OBCCBO is the most stable structure among the three isomers. The OBBCCO and OCBBCO structures were predicted to be 35.0 and 94.9 $kcal\,mol^{-1}$ less stable than OBCCBO, respectively, at the B3LYP6-311+G* level of theory. Recent studies showed that C_nBO and OC_nB ($n=2$ or 4) are linear molecules with the C_nBO structures being more stable than the OC_nB isomers. The rearrangement reactions from the C_nBO species to OC_nB are endothermic and require significant activation energies.[33]

The formation of OBBCCO, and in particular OBCCBO, from the reactions of boron atoms with carbon monoxide is of great interest. The optimized geometries of OBBCCO and OBCCBO calculated at the B3LYP level are in excellent agreement with those calculated at the CCSD(T) level, as shown in Figure 6. The OBBCCO molecule involves a C–C double bond. The C=C bond length was predicted to be 1.289 Å (B3LYP) or 1.303 Å (CCSD(T)). The Lewis structure is best described as O≡B–B=C=C=O. The OBCCBO molecule involves a C–C triple bond. The C≡C bond length was computed to be 1.212 Å (B3LYP), slightly longer than that of C_2H_2 (1.199 Å) calculated at the same level of theory. The Lewis structure of OBCCBO can be drawn as O≡B–C≡C–B≡O, a polyyne-like structure, which satisfies the octet rule. Just as the N_2 molecule can be seen as the neutral dipnictide, corresponding to two nitride anions, N^{3-}, the present OCBBCO and OBCCBO species can be seen as the neutral dipseudopnictides, whose closed-shell monomers are OCB^{3-} and OBC^{3-}, respectively. The latter was predicted to lie at a lower energy.[34] The asymmetrical OBBCCO species could alternatively be seen as OB-BCCO. The pseudohalide $BCCO^-$ seems new, its close neighbors in the dicyanogen isoelectronic series and the pseudohalide BO^- have been discussed.[35]

Although the other boron carbonyl absorption bands BCO, BBCO, and $B(CO)_2$ also decreased or disappeared on broad-band irradiation, no photo-induced rearrangement products such as CBO and OBCCO were observed. These carbonyl species probably decomposed, as the CO absorption band at 2138.3 cm^{-1} greatly increased on broad-band irradiation.

Conclusion

The co-deposition of laser-ablated boron atoms with CO molecules in solid argon formed the following boron carbonyl species (which have been reported earlier): BCO, BBCO, OCBBCO, $B(CO)_2$, and $B_4(CO)_2$. The OCBBCO molecule, which exhibits some boron–boron triple-bond character, underwent successive photochemical rearrangements to form the OBBCCO isomer and finally the OBCCBO structure, which provides an unprecedented mechanism for CO activation. The new molecules were identified on the basis of isotopic IR studies with ^{10}B, ^{11}B, $^{13}C^{16}O$, $^{12}C^{18}O$, and carbon monoxide mixtures in addition to comparison with quantum-chemical calculations of isotopic frequencies. The theoretical analyses found that OBBCCO and OBCCBO are linear molecules with C–C double and triple bonding, and lie much lower in energy than the linear OCBBCO isomer. The stabilities of the three $B_2C_2O_2$ isomers increase as OCBBCO < OBBCCO < OBCCBO.

Acknowledgement

We thank the referees for helpful discussions. This work is supported by the National Science Foundation of China (NSFC grant 20125311), the National Key Basic Research Special Foundation (NKBRSF) of China, the Japan Society for the Promotion of Science (JSPS) and the New Energy and Industrial Technology Development Organization (NEDO) of Japan.

[1] See, for example: a) E. L. Muetterties, J. Stein, *Chem. Rev.* **1979**, *79*, 479; b) K. Tatsumi, A. Nakamura, P. Hoffmann, P. Stauffert, R. Hoffmann, *J. Am. Chem. Soc.* **1985**, *107*, 4440.
[2] M. F. Zhou, L. Andrews, C. W. Bauschlicher, Jr., *Chem. Rev.* **2001**, *101*, 1931, and references therein.
[3] a) M. F. Zhou, L. Andrews, J. Li, B. E. Bursten, *J. Am. Chem. Soc.* **1999**, *121*, 12188; b) J. Li, B. E. Bursten, M. F. Zhou, L. Andrews, *Inorg. Chem.* **2001**, *40*, 5448.
[4] M. F. Zhou, L. Andrews, J. Li, B. E. Bursten, *J. Am. Chem. Soc.* **1999**, *121*, 9712.
[5] M. F. Zhou, L. Andrews, *J. Phys. Chem. A* **1999**, *103*, 7785.
[6] M. F. Zhou, L. Andrews, *J. Am. Chem. Soc.* **2000**, *122*, 1531.
[7] A. J. Hinchcliffe, J. S. Ogden, D. D. Oswald, *J. Chem. Soc. Chem. Commun.* **1972**, 338.
[8] a) P. H. Kasai, P. M. Jones, *J. Am. Chem. Soc.* **1984**, *106*, 8018; b) P. H. Kasai, P. M. Jones, *J. Phys. Chem.* **1985**, *89*, 2019; c) W. G. Hatton, N. P. Hacker, P. H. Kasai, *J. Phys. Chem.* **1989**, *93*, 1328.
[9] a) J. H. B. Chenier, C. A. Hampson, J. A. Howard, B. Mile, R. Sutcliffe, *J. Phys. Chem.* **1986**, *90*, 1524; b) J. H. B. Chenier, C. A. Hampson, J. A. Howard, B. Mile, *J. Chem. Soc. Chem. Commun.* **1986**, 730.
[10] Y. M. Hamrick, R. J. Van Zee, J. T. Godbout, W. Weltner, W. J. Lauderdale, J. F. Stanton, R. Bartlett, *J. Phys. Chem.* **1991**, *95*, 2840.
[11] T. R. Burkholder, L. Andrews, *J. Phys. Chem.* **1992**, *96*, 10195.
[12] C. Xu, L. Manceron, J. P. Perchard, *J. Chem. Soc. Faraday Trans.* **1993**, *89*, 1291.
[13] H. J. Himmel, A. J. Downs, J. C. Green, T. M. Greene, *J. Phys. Chem. A* **2000**, *104*, 3642.
[14] L. N. Zhang, J. Dong, M. F. Zhou, Q. Z. Qin, *J. Chem. Phys.* **2000**, *113*, 10169.
[15] V. Balaji, K. K. Sunil, K. D. Jordan, *Chem. Phys. Lett.* **1987**, *136*, 309.
[16] a) A. Skancke, J. F. Liebman, *J. Phys. Chem.* **1994**, *98*, 13215; b) B. S. Jursic, *Chem. Phys.* **1997**, *219*, 57.
[17] a) S. S. Wesolowski, T. D. Crawford, J. T. Fermann, H. F. Schaefer, *J. Chem. Phys.* **1996**, *104*, 3672; b) S. S. Wesolowski, J. M. Galbraith, H. F. Schaefer, *J. Chem. Phys.* **1998**, *108*, 9398.
[18] a) A. J. Bridgeman, *J. Chem. Soc. Dalton Trans.* **1997**, 1323; b) A. J. Bridgeman, *Inorg. Chim. Acta* **2001**, *321*, 27.
[19] M. F. Zhou, Z. X. Wang, P. von R. Schleyer, Q. Xu, *ChemPhysChem* **2003**, *4*, 763.
[20] M. F. Zhou, N. Tsumori, Z. H. Li, K. N. Fan, L. Andrews, Q. Xu, *J. Am. Chem. Soc.* **2002**, *124*, 12936.
[21] M. F. Zhou, Q. Xu, Z. X. Wang, P. v. R. Schleyer, *J. Am. Chem. Soc.* **2002**, *124*, 14854.
[22] a) G. H. Robinson, *Acc. Chem. Res.* **1999**, *32*, 773; b) P. P. Power, *Chem. Rev.* **1999**, *99*, 3463; c) J. R. Su, X.-W. Li, R. C. Crittendon, G. H. Robinson, *J. Am. Chem. Soc.* **1997**, *119*, 5471; d) Y. Xie, R. S. Grev, J. D. Gu, H. F. Schaefer, P. von R. Schleyer, J. R. Su, X. W. Li, G. H. Robinson, *J. Am. Chem. Soc.* **1998**, *120*, 3773; e) F. A. Cotton, A. H. Cowley, X. J. Feng, *J. Am. Chem. Soc.* **1998**, *120*, 1795; f) Y. Xie, H. F. Schaefer, G. H. Robinson, *Chem. Phys. Lett.* **2000**, *317*, 174; g) K. W. Klinkhammer, *Angew. Chem.* **1997**, *109*, 2414; *Angew. Chem. Int. Ed. Engl.* **1997**, *36*, 2320; h) I. Bytheway, Z. Lin, *J. Am. Chem. Soc.* **1998**, *120*, 12133.
[23] a) T. R. Burkholder, L. Andrews, *J. Chem. Phys.* **1991**, *95*, 8697; b) M. H. Chen, X. F. Wang, L. N. Zhang, M. Yu, Q. Z. Qin, *Chem. Phys.* **1999**, *242*, 81.
[24] DFT and CCSD(T) calculations were performed by using Gaussian 98 (Revision A.7), M. J. Frisch, G. W. Trucks, H. B. Schlegel, G. E. Scuseria, M. A. Robb, J. R. Cheeseman, V. G. Zakrzewski, J. A. Montgomery, Jr., R. E. Stratmann, J. C. Burant, S. Dapprich, J. M. Millam, A. D. Daniels, K. N. Kudin, M. C. Strain, O. Farkas, J. Tomasi, V. Barone, M. Cossi, R. Cammi, B. Mennucci, C. Pomelli, C. Adamo, S. Clifford, J. Ochterski, G. A. Petersson, P. Y. Ayala, Q. Cui, K. Morokuma, D. K. Malick, A. D. Rabuck, K. Raghavachari, J. B. Foresman, J. Cioslowski, J. V. Ortiz, B. B. Stefanov, G. Liu, A. Liashenko, P. Piskorz, I. Komaromi, R. Gomperts, R. L. Martin, D. J. Fox, T. Keith, M. A. Al-Laham, C. Y. Peng, A. Nanayakkara, C. Gonzalez, M. Challacombe, P. M. W. Gill, B. G. Johnson, W. Chen, M. W. Wong, J. L. Andres, M. Head-Gordon, E. S. Replogle, J. A. Pople, Gaussian, Inc., Pittsburgh, PA, **1998**.
[25] A. D. Becke, *J. Chem. Phys.* **1993**, *98*, 5648.
[26] C. Lee, E. Yang, R. G. Parr, *Phys. Rev. B* **1988**, *37*, 785.
[27] J. A. Pople, M. H. Gordon, K. Raghavachari, *J. Chem. Phys.* **1987**, *87*, 5968.
[28] a) A. D. McLean, G. S. Chandler, *J. Chem. Phys.* **1980**, *72*, 5639; b) R. Krishnan, J. S. Binkley, R. Seeger, J. A. Pople, *J. Chem. Phys.* **1980**, *72*, 650.
[29] M. F. Zhou, N. Tsumori, L. Andrews, Q. Xu, *J. Phys. Chem. A* **2003**, *107*, 2458.
[30] R. D. Brown, D. E. Pullin, E. H. N. Rice, M. Rodler, *J. Am. Chem. Soc.* **1985**, *107*, 7877.
[31] The optimized structure of BOBCCO: B–O 1.309, O–B 1.323, B–C 1.340, C–C 1.281, C–O 1.161 Å; this molecule has two strong C–O stretching and B–O–B stretching modes at 2301.4 (2489 km mol^{-1}) and 1515.4 cm^{-1} (1162 km mol^{-1}); although the 2301.4 cm^{-1} band matches the observed frequency, the spectrum in the 1600–1400 cm^{-1} region is very clean and no band was observed. The optimized structure of OBCBCO: O–B 1.211, B–C 1.470, C–B 1.322, B–C 1.437, C–O 1.141 Å; the molecule was calculated to have a strong C–O stretching mode at 2221.2 cm^{-1} with isotopic frequency ratios of $^{10}B/^{11}B$ 1.0057, $^{12}C/^{13}C$ 1.0248, and $^{16}O/^{18}O$ 1.0157, which do not fit the experimental values.
[32] See, for example: I. Bytheway, M. W. Wong, *Chem. Phys. Lett.* **1998**, *282*, 219.
[33] a) A. M. McAnoy, S. Dua, D. Schroder, J. H. Bowie, H. Schwarz, *J. Phys. Chem. A* **2003**, *107*, 1181; b) A. M. McAnoy, S. Dua, D. Schroder, J. H. Bowie, H. Schwarz, *J. Phys. Chem. A* **2004**, *108*, 2426.
[34] P. Pyykko, Y. F. Zhao, *J. Phys. Chem.* **1990**, *94*, 7753.
[35] a) P. Pyykko, N. Runeberg, *J. Mol. Struct.* **1991**, *234*, 269; b) P. Pyykko, *Mol. Phys.* **1989**, *67*, 871.

Received: May 14, 2004
Published online: October 7, 2004

